Histochemistry and Cell Biology (2018) 150:173–185
https://doi.org/10.1007/s00418-018-1682-9

ORIGINAL PAPER

Dynamic of VE-cadherin-mediated spermatid–Sertoli cell contacts in the mouse seminiferous epithelium

Giovanna Berruti[1] · **Michela Ceriani**[2] · **Enzo Martegani**[2]

Accepted: 18 May 2018 / Published online: 25 May 2018

Abstract

Spermatids are haploid differentiating cells that, in the meantime they differentiate, translocate along the seminiferous epithelium towards the tubule lumen to be just released as spermatozoa. The success of such a migration depends on dynamic of spermatid–Sertoli cell contacts, the molecular nature of which has not been well defined yet. It was demonstrated that the vascular endothelial cadherin (VEC) is expressed transitorily in the mouse seminiferous epithelium. Here, we evaluated the pattern of VEC expression by immunohistochemistry first in seminiferous tubules at different stages of the epithelial cycle when only unique types of germ cell associations are present. Changes in the pattern of VEC localization according to the step of spermatid differentiation were analysed in detail using testis fragments and spontaneously released germ cells. Utilizing the first wave of spermatogenesis as an in vivo model to have at disposal spermatids at progressive steps of differentiation, we checked for level of looser VEC association with the membrane by performing protein solubilisation under mild detergent conditions and assays through VEC-immunoblotting. Being changes in VEC solubilisation paralleled in changes in phosphotyrosine (pY) content, we evaluated if spermatid VEC undergoes Y658 phosphorylation and if this correlates with VEC solubilisation and spermatid progression in differentiation. Altogether, our study shows a temporally restricted pattern of VEC expression that culminates with the presence of round spermatids to progressively decrease starting from spermatid elongation. Conversely, pY658-VEC signs elongating spermatids; its intracellular polarized compartmentalization suggests a possible involvement of pY658-VEC in the acquisition of spermatid cell polarity.

Keywords Spermiogenesis · Cell polarity · Male fertility · Rap1 · Tyrosine phosphorylation

Introduction

Spermiation is the final stage of spermiogenesis and is the process through which mature spermatids acquire their final remodeling and detach from the supporting Sertoli cells to be released as spermatozoa into the tubule lumen. This final release of spermatids is a process dependent from the action of estrogen and androgen and is particularly sensitive to hormone suppression (Nicholls et al. 2011). To reach the luminal edge, spermatids have to migrate across the length of the seminiferous epithelium, i.e. from the basal to the adluminal compartment (Xiao et al. 2014; Berruti and Paiardi 2014; Wen et al. 2016). This is an unusual movement for cells like spermatids that are considered immotile; it is, thus, generally accepted that spermatid migration is realized by relying on the restructuring of spermatids–Sertoli cells contacts (Vogl et al. 2000; Xiao et al. 2014; Berruti and Paiardi 2014; Wen et al. 2016). One of the most representative of these cell–cell contacts is a hybrid anchoring junction known as apical ectoplasmic specialization (aES); through aES, in the mouse, Sertoli cells interact with spermatids at steps 7 of their differentiation to persist in interaction till spermatids reach the final step 16, just before spermiation (Vogl et al. 2000; O'Donnell et al. 2011; Xiao et al. 2014). At the beginning of spermiation, aES disassembles while tubulobulbar complexes (TBCs) do their appearance

Electronic supplementary material The online version of this article (https://doi.org/10.1007/s00418-018-1682-9) contains supplementary material, which is available to authorized users.

✉ Giovanna Berruti
giovanna.berruti@unimi.it

[1] Department of Biosciences, University of Milan, Via Celoria 26, 20133 Milan, Italy

[2] Department of Biotechnology and Biosciences, University of Milano-Bicocca, Milan, Italy

(Guttman et al. 2004). These last are enigmatic structures resembling podosomes, which have been proposed as subcellular machines responsible for internalizing intact aES inside Sertoli cells during sperm release (Guttman et al. 2004; Young et al. 2009; O'Donnell et al. 2011). Notwithstanding the recent progresses in understanding the nature and structure of the cell adhesion molecules involved in spermatid–Sertoli cell contacts (Mullholland et al. 2001; Berruti and Paiardi 2014; Wen et al. 2016), several unresolved questions remain, in particular about the aES. It is not definitely unravelled yet, for example, which are the protein complexes, i.e. the adhesion molecules with associated structural and signalling components, that regulate the formation, assembly, stability, dynamic, and/or disassembling of the aES, respectively. The heterogeneity emerged from various studies regarding the structural components of this testis-specific junction does not help in fact in clarifying which are the molecular players involved in a definite step (aES formation, stabilization, destabilization). Components of aES include cadherins/catenins (Mullholland et al. 2001; Johnson and Boekelheide 2002; Domke et al. 2014; Li et al. 2015) and nectin/afadin complexes (Ozaki-Kuroda et al. 2002; Inagaki et al. 2006), typical of adherens junctions, as well as junction adhesion molecule complexes (Gliki et al. 2004), typical of tight junctions, and integrin/laminin complexes (Cheng et al. 2011a; Domke et al. 2014), typical of focal contacts. Among the members of the cadherin superfamily, there is VE-cadherin (VEC) (Cadwell et al. 2016). VEC, originally named cadherin 5 (Suzuki et al. 1991), gives its actual name because it is predominant in endothelial cells (Bravi et al. 2014), but it is expressed also in other cells (Combes et al. 2009; Bartolomé et al. 2017) including spermatids and Sertoli cells (Aivatiadou et al. 2007). More specifically, in the testis VEC shows a stage-specific pattern of expression varying according to the phase/s of the seminiferous epithelial cycle (Aivatiadou et al. 2007). Generally speaking VEC, which is a single-pass transmembrane protein, associates through its carboxy terminus with cytoplasmic proteins of the armadillo family, like p120-catenin, b-catenin and plakoglobin, thus contributing to the stability of VEC-mediated cell contacts (Giampietro 2016). Furthermore, the interaction of VEC with p120-catenin is critical for actin cytoskeleton organization (Xiao et al. 2005). To supervise all these events there is the small GTPase Rap1 that acts as crucial mediator of junction stability and organizer of cell architecture (Berruti 2000; Kooistra et al. 2007; Wilson and Ye 2014; Lakshmikanthan et al. 2015). The disruption of VEC-mediated contacts, on the other hand, is regulated by a series of events that lead to VEC phosphorylation and endocytosis and/or intramembrane cleavage (Xiao et al. 2005; Wilson and Ye 2014; Lakshmikanthan et al. 2015). Here, it is another Ras-like small GTPase, Rho, to play a crucial role; Rho is in fact best known as counter-actor of the action of Rap1 (Aivatiadou et al. 2009; Di Lorenzo et al. 2013; Pronk et al. 2017).

Upon the grounds of these considerations, in the present study we have extended the preliminary characterization on VEC in the mouse seminiferous epithelium (Aivatiadou et al. 2007) by examining in detail VEC cellular localization and distribution. Further, we have searched for tyrosine-phosphorylated VEC, namely pY_{658}-VEC, which is the phosphorylated form that hallmarks dissociation of VEC from p120-catenin allowing its binding to polarity proteins (Conway et al. 2017). Lastly, we verified whether there is a relation, if any, between variation in VEC plasma membrane level/pY_{658}-VEC phosphorylation and the events that precede spermiation. A brief report about this topic was presented in preliminary form elsewhere (19th European Testis Workshop, S. Malò, 2016).

Materials and methods

Animals

CD1 male mice were purchased from Charles River Italia (Calco, Lecco, Italy) and housed with ad libitum access to food and water at a temperature of 21 ± 1 °C with a relative humidity of $55 \pm 10\%$ and 12-h light/dark cycle. Animals, used as organ donors, were killed by carbon dioxide asphyxiation at the selected time as indicated. All efforts were made to minimize the number of animals used. Animal protocols used were carried out with authorization by the ethical committee for animal experimentation of University of Milan and by the Italian Ministry of Health and were in compliance with the animal care requirements (Italian law D.L. 27.1.1992 n. 116, in agreement with the European Union directive 86/609/CEE) and NIH Guide for the Care and Use of Laboratory Animals.

Antibodies

Primary antibodies, listed below, were obtained commercially as purified IgGs, except for anti-pY658 VEC that was a generous gift by E. Dejana, University of Milan; anti-pY658 VEC has been characterized previously (Orsenigo et al. 2012). Anti-VE cadherin (VEC) antibodies were: goat anti-VEC (sc-64,581, Santa Cruz Biotechnology, Santa Cruz, CA, USA) and rabbit anti-VEC (36-1900, Thermo Fisher Scientific, Rockford, IL, USA). Mouse monoclonal anti-SP56 (clone 7C5, MA1-10866) was from Thermo Fisher Scientific (USA). Secondary antibodies were: anti-goat and anti-rabbit horseradish peroxidase-conjugated IgGs (GE Healthcare, UK), anti-goat and anti-rabbit IgGs Alexa

Fluor 488 and anti-mouse IgGs Alexa Fluor 568 (Invitrogen, Thermo Fisher Scientific, USA).

Histology and immunohistochemistry

Testes were removed, fixed, and processed for peroxidase-based immunohistochemistry essentially as previously reported (Aivatiadou et al. 2007; Paiardi et al. 2014), including sections obtained from paraffin-embedded testes of iRap1 transgenic mice (Aivatiadou et al. 2007). Endogenous peroxidase activity was quenched in 0.3% H_2O_2 for 10 min and sections, treated first with primary antibody and then with horseradish peroxidase-conjugated secondary antibody, were processed for staining with the Vector NovaRED substrate kit for peroxidase (Vector Laboratories. Burlingame, CA, USA). Sections were counterstained with haematoxylin (Vector Laboratories). In controls, primary antibody was replaced with goat normal serum. Tubules were classified into the specific stages according to the classification of Oakberg (1956). Testis immunofluorescence analysis was performed using both paraffin-embedded sections and cryosections; the first were processed as already described (Aivatiadou et al. 2007; Paiardi et al. 2011; Berruti and Paiardi 2015), with nuclei counterstaining carried out with 4′,6-diamidino-2-phenylindole (DAPI; 2 µg/ml, Sigma-Aldrich Chemical Company) or Draq5 (5 µM, Biostatus Limited, Shepshed, UK). For cryosections, testes were immediately submerged in OCT compound (Sekura Finetek Inc., Torrance, CA, USA) and frozen using liquid nitrogen. Frozen sections (7 µm) were cut on a cryomicrotome, collected on poly-L-lysine-coated slides and immediately fixed into cold (− 20 °C) acetone for 5 min. After further 5 min into cold (− 20 °C) methanol, the slides were removed from the methanol, air dried and then processed for VEC-immunostaining. Incubations with the appropriate Alexa 488-conjugated secondary antibodies followed the incubations with primary antibodies. In control samples, the primary antibodies were either omitted or replaced with normal goat serum.

For single immunohistochemical analysis, the samples were analysed under an Axiovert 200 M inverted microscope (Zeiss Microscopy GmbH, Jena, Germany), equipped with bright-field light optics and standard filter sets for green (Alexa Fluor 488), red (Alexa Fluor 568) and blue (DAPI) fluorescence and a Zeiss AxioCam, CCD camera. Some samples were examined also at the confocal microscopy (see below). Acquired images were elaborated with Adobe Photoshop (Mountain View, CA, USA).

Fragmented material and immunofluorescence

Fragmented material was obtained according to a slightly modified procedure by Guttman et al. (2004). Briefly, testes were decapsulated in PBS (150 mM NaCl, 5 mM KCl, 0.8 mM KH_2PO_4, 3.2 mM Na_2HPO_4, pH 7.3) and the seminiferous tubule mass was rapidly cut into small pieces that were then fixed in 4% (v/v) paraformaldehyde for 2 h at 4 °C. The pieces were transferred into a 15-ml plastic Falcon tube along with about 5 ml of PBS and gently aspirated through an 18-gauge, and then a 21-gauge needle attached to a 10-ml syringe, for 3–5 passes/each. This fragmented material was left to sediment for 5 min at room temperature so that larger tubule fragments settled to the bottom of the tube. Smaller epithelial fragments, remained suspended in solution, were removed and transferred into another 15-ml tube and centrifuged at low speed (350×*g*) to pellet the epithelial fragments. The supernatant was removed and further processed as described below, while the pellet was gently resuspended in Tris-buffered saline (TBS), pH 7.4. These fragments were then transferred to poly-L-lysine-coated slides and allowed to incubate in a humidity chamber for 10 min. After remotion of the excess fluid, slides were submerged for few seconds in cold acetone (− 20 °C) and then in cold methanol (− 20 °C) for 5 min and allowed to air dry. The low-speed supernatant, transferred in another tube, was centrifuged at higher speed (850x*g*) to recover the germ cells spontaneously released from the fragments in consequence of the treatment. The pelleted cells were gently resuspended in a low volume of TBS buffer, smeared on a glass slide, post-fixed in ice-cold methanol for 5 min, air-dried and rehydrated. All the buffers used when released cells had to be processed for pY658 immunolabeling were added with 100 µM vanadate and 200 µM hydrogen peroxide. Rehydrated tissue fragments and released cells were therein processed for immunofluorescence essentially as described previously (Berruti and Paiardi 2015). Before the blocking step in 3% BSA, some slides with attached tissue fragments were pre-incubated in 0.2% Triton X-100 for 10 min. Indicated primary antibodies, that is, goat anti-VEC (1:75), rabbit anti-VEC (1:50), rabbit anti-pY658 VEC (1:25), and mouse anti-sp56 (1:250) were followed by the appropriate Alexa 488- and/or Alexa 568-conjugated secondary antibodies. Nuclei counterstaining was carried out with DAPI (2 µg/ml). Samples were examined on a Leica TCS SPAOBS scanning laser confocal fluorescent microscope (Leica Lasertecknik GmbH, Heidelberg, Germany) equipped with laser Ar/Kr (488 nm), laser He/Ne (568 nm), and laser UV (361–365 nm) for green, red, and blue fluorescence, respectively. Images, including the controls, were captured under 63X magnification using identical laser power, light pathways and band passes

by a computerized system (Leica Power Scan software). Captured images were elaborated with Adobe Photoshop (Mountain View, CA, USA).

Protein extracts, protein partition, immunoprecipitation, and western blot analysis

Seminiferous tubules were isolated from 25-day-old and 32-day-old testes following a slightly modified procedure from that used previously (Aivatiadou et al. 2007). Briefly, a small aliquot of decapsulated testis was withdrawn and directly incubated in the detergent buffer (see below) to be homogenized in a siliconized glass microhomogenizer. The clarified lysate from testis homogenate is the total homogenate fraction. The remaining seminiferous tubule mass was processed for enzymatic digestion using collagenase (0.05%, wt/vol) under gentle shaking for 6–7 min, at 34 °C. The collagenase solution was then withdrawn by decantation and the interstitial cells were removed with washings in RPMI 1640 medium (Gibco, Thermo Fisher) by sedimentation under unit gravity at room temperature. For partitioning into VEC soluble and insoluble fractions, the washed seminiferous tubules were pelleted by centrifugation at 200x*g*, resuspended in homogenizing buffer (10 mM Tris, 150 mM NaCl, pH 7.5, containing 0.1% Triton X-100 plus a complete protease inhibitor cocktail from Sigma-Aldrich, St Louis, MO, USA) and immediately transferred to a siliconized glass microhomogenizer to be thoroughly homogenized on ice. The resulting lysates, clarified by centrifugation for 10 min at 12,000x*g*, 4 °C, and concentrated, are the soluble VEC fraction. The respective pellets were, in turn, resuspended in the detergent buffer (10 mM Tris, 150 mM NaCl, pH 7.5, plus 0.5% Triton X-100, 0.5% Nonidet NP40, and 0.1% SDS [wt/vol] as final concentrations and the complete cocktail of protease inhibitors), shaken and allowed to continue on a rotating platform for 20 min at 4 °C. The detergent extracts, clarified by centrifugation, are the VEC insoluble fraction. Protein concentration was determined using a protein assay (Bio-Rad DC Protein Assay, Bio-Rad, Hercules, CA, USA). Same protein amounts (100 µg) of VEC-soluble and -insoluble fractions were loaded and run on SDS-polyacrylamide gels.

For immunoprecipitation, the procedure described previously was followed (Aivatiadou et al. 2007). Briefly, after collagenase digestion seminiferous tubules from 25-day-old and 32-day-old testes were washed four times with RPMI 1640 medium containing 100 µM vanadate and 200 µM hydrogen peroxide. Extraction buffer, i.e. the detergent buffer reported above, and all the subsequent buffers used contained in addition 300 µM vanadate and 600 µM hydrogen peroxide. For each immunoprecipitation (IP) assay, 800 µg of seminiferous tubule protein lysate was incubated with anti-pY658 VEC antibody for 2 h at 4 °C on a rotating platform, followed by a 1-h incubation in protein A/G agarose (Pierce, Thermo Fisher) under the same conditions. Control samples received the preimmune serum. After two washings with IP buffer and further two washings with cold 10 mM Tris–HCl, 150 mM NaCl, pH 7.4, containing vanadate and hydrogen peroxide, the precipitated immunocomplexes were resuspended in 2X SDS-polyacrylamide gel electrophoresis (PAGE) sample buffer, and the eluted bound proteins were resolved on SDS-PAGE. Electrophoresed proteins were subjected to Western blotting and immunodecorated with anti-VE cadherin antibodies using standard protocols.

After immunoblotting, Image J software was used to quantify the intensity of immunoreactive protein bands, and data were expressed as arbitrary units of pixel density following normalization on respective total VEC.

Results

VEC in the seminiferous epithelium

The first report on the presence of VEC in the adult seminiferous epithelium was in a work devoted to the generation and characterization of transgenic mice that express an inactive dominant variant of Rap1 specifically in spermatids (Aivatiadou et al. 2007). Further information being missing, here we investigated in detail the presence of VEC in wild-type mice.

By peroxidase-immunohistochemistry carried out on testis sections, a strong VEC-immunopositivity was revealed in spermatids at stages V–VI–VII of the epithelial cycle (Fig. 1, compare with the respective controls). At these magnifications that provide a general view of a testis cross section, it is difficult to visualize clearly the cellular bodies; enlargements (Fig. 1, right side), however, allow of appreciating that at the adluminal compartment the cellular bodies of elongating spermatids that grasp at the branches of the supporting Sertoli cells are highly VEC-immunostained, while at the basal compartment the bodies of Sertoli cells stand out for their VEC-positivity. Spermiation is a protracted process that in the mouse begins at early stage VIII to complete at the end of stage VIII. VEC immunostaining was found to decrease remarkably at early spermiation to disappear at the adluminal compartment at late stage VIII; the basally located Sertoli's cell bodies remained, however, always VEC-immunopositive (Fig. 2a). These findings confirm more in detail what was described previously (Aivatiadou et al. 2007). VEC-localization on testis sections was assayed also by immunofluorescence. This analysis provided essentially results similar to peroxidase-immunohistochemistry (Fig. 2b, b', stage VI). Immunofluorescence, however, allowed visualizing sharply also the cellular profiles; so,

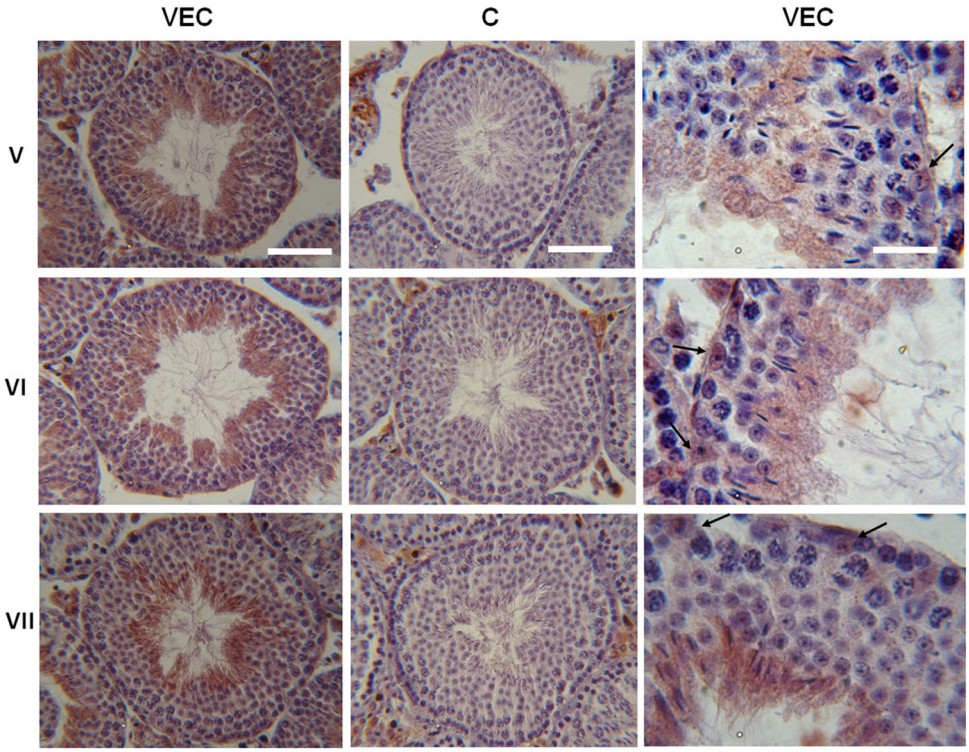

Fig. 1 VEC expression at different stages of the seminiferous epithelial cycle. Representative cross sections at stages V, VI, VII, immune-peroxidase stained for VEC and counterstained with haematoxylin to appreciate the chromatin patterns. These stages (each for strip) comprise specific cell–cell associations with post-meiotic germ cells undergoing differentiation from round spermatids at step 5, when aES has not appeared yet, to elongated spermatids at step 16, when aES is dismantled. Left column: VEC-immunopositivity marks in particular post-meiotic cells (Stage V, spermatids at steps 5–15; Stage VI, spermatids at steps 6–15; Stage VII, spermatids at steps 7–16). Bar = 50 µm. Middle column (C): controls, the omission of primary antibodies documents the lack of VEC-immunostaining in the seminiferous epithelium. Only interstitial cells exhibit aspecific positivity to peroxidase-conjugated secondary antibodies. Bar = 50 µm. Right column: enlargements that well visualize the VEC positivity including the Sertoli cell bodies (arrows) at the basal compartment. Bar = 20 µm

the contours of round spermatids resulted to be strongly VEC-immunopositive (Fig. 2c, c', stage VII and Supplementary Fig. 1). This was particularly evident when VEC immunostaining was carried out on cryosections (Fig. 3). To resolve further the cellular profiles, we resorted to analyse fragments of seminiferous epithelium dissociated mechanically, i.e. without any enzymatic treatment, (Gutmann et al. 2004). A sharp VEC-immunosignal was detected at the cellular contours of the cohorts of round spermatids maintained in a context of organ architecture, independently if subjected or not to Triton X-100 pre-treatment (Fig. 4a, b); no specific staining was observed when VEC antibodies were replaced with normal goat serum (not shown). Lastly, since spermatids can be spontaneously released from the fragmented seminiferous tubules (Gutman et al. 2004), we recovered the released cells for immunostaining. Even under these conditions, isolated round spermatids showed VEC-immunopositivity at the plasma membrane level (Fig. 4c, d). We can conclude that VEC is a surface component in early differentiating mouse spermatids.

VEC relocation and internalization in elongating spermatids

One of aES major functions is to maintain the attachment of developing spermatids on the Sertoli cell concomitantly to spermatid migration across the seminiferous epithelium (Vogl et al. 2000; Xiao et al. 2014; Wen et al. 2016). As said, aES starts to develop with mouse spermatids at step 7 to persist till to spermatid at step 16. During their differentiation spermatids acquire a highly polarized cell shape and their correct arrangement within the seminiferous epithelium implies that they have to be packed with the spermatid heads pointed toward the basement membrane and the tails towards the tubule lumen. We were thus interested to check for the behaviour of VEC when such morphogenetic cell differentiation is occurring. It is known that aES opposes apically the developing spermatid acrosome (Russell et al. 1983). Therefore, to identify the apical region, we performed a double immunofluorescence labelling, i.e. in addition to VEC, we immunolabeled spontaneously released spermatids with

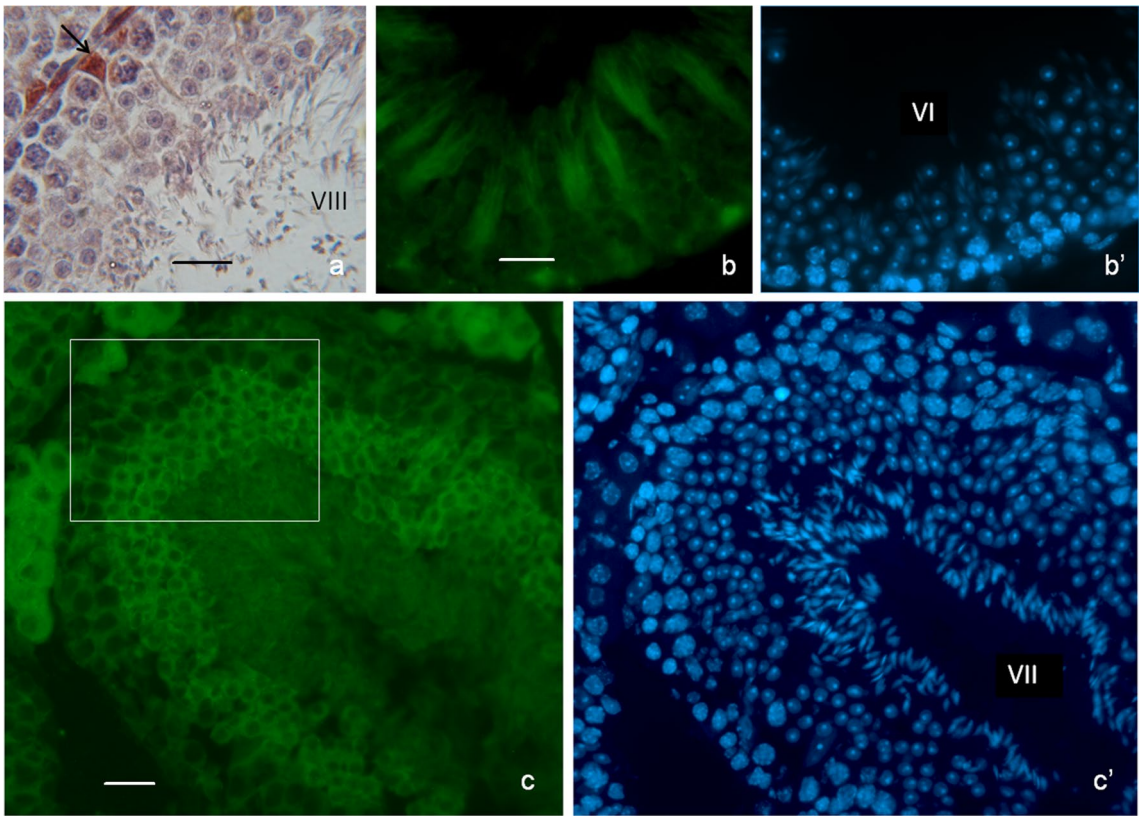

Fig. 2 VEC localization in paraffin-embedded testes by immune-peroxidase and immune-fluorescence analyses. **a** A particular of a peroxidase-stained cross section at stage VIII showing that at spermiation, Sertoli cells only are VEC-immunopositive in the seminiferous epithelium. Bar = 15 µm. **b** and **c** VEC immunofluorescence: the focal planes enlighten the VEC staining of elongating spermatid bodies that grasp at the branches of the supporting Sertoli cells (**b**, stage VI) and of round spermatid cellular profiles (**c**, stage VII). The boxed area in **c** is provided as enlargement in Supplemental Fig. 1. **b', c'**: the respective DAPI counterstaining. Bar = 20 µm for **b** and **c**

antibodies against sp56, a marker of the acrosome development (Berruti and Paiardi 2015). By exploiting the pattern of sp56 immunolabeling, it was confirmed that VEC immunostaining signs uniformly the cell surface of round spermatids at the so-called Golgi phase when aES assembling is not started yet (Fig. 5, column a) as well as of round spermatids at early and late cap phase when aES formation is started and mostly developed, respectively (Fig. 5, columns b and c). An unexpected situation was, however, revealed in spermatids at more advanced stages of differentiation. In spermatids at the acrosomal phase (Fig. 5d, asterisk), the association of VEC with the cellular surface failed at the apical region where aES is depicted to be stabilized, whereas it persisted in other regions of the cellular surface. Moreover, starting from these spermatids characterized by a cytoplasm that is going to concentrate at the distal pole, VEC staining marked also the polarized cytoplasm (Fig. 5d). At more advanced maturation steps, concomitantly with the progression of spermatid elongation and acrosome flattening, VEC was still more caudally compartmentalized, being confined to the cytoplasm around the top of the flagellum (Fig. 5d); its surface labeling disappeared at all. These findings suggest that spermatid–Sertoli cell contacts take place first through VEC engagement along the entire round spermatid surface. The successive decrease of VEC-mediated cell contacts, starting from the region where aES is commonly described to be well established (Vogl et al. 2000; Cheng et al. 2011a, b), and the parallel increase of VEC inside the spermatid cytoplasm suggest the occurrence of internalization and intracellular trafficking of the cadherin.

Evidence in support of this interpretation comes from iRap1 transgenic mice. When we assayed iRap1 testes by immunohistochemistry, VEC immunostaining was found inside the round spermatids prematurely released into the tubule lumen (Fig. 6, asterisk in both immunofluorescence and immunoperoxidase labeling); even when still in situ, early spermatids from the transgenic testis showed cytoplasm positive to VEC (Fig. 6). The loss of VEC–plasma membrane association in iRap1 round spermatids, contrary to the VEC surface labeling in wild-type spermatids, is consistent with what was described to occur when Rap1 is silenced in somatic cells (Noda et al. 2010; Wilson and

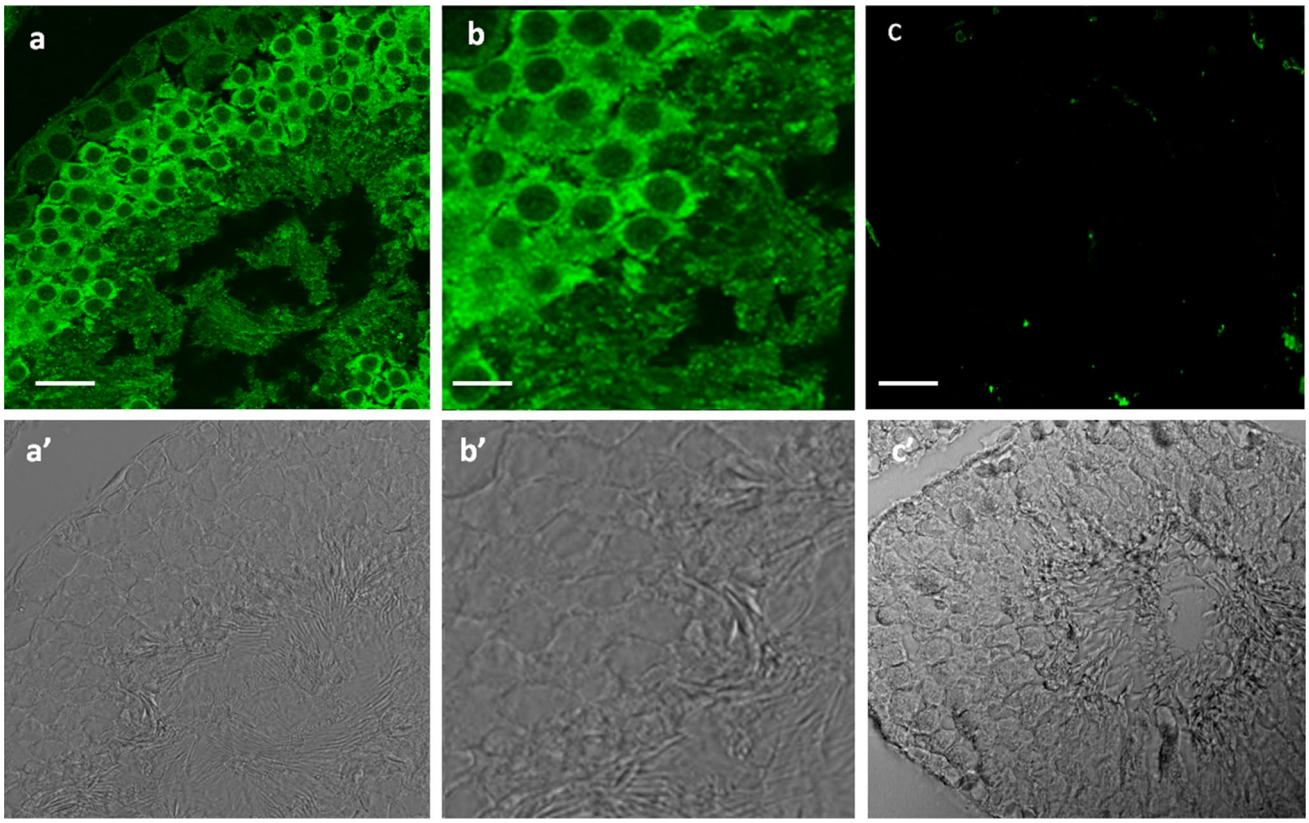

Fig. 3 VEC localization in testis cryo-sections. **a** VEC immunopositivity at the cellular contours of round spermatids is evidenced in cryosections of seminiferous epithelium (compare with **c**, the control). **b** Enlargement revealing a dotted thread-like labelling along the positive cellular profiles; positive spots can be occasionally observed inside the cytoplasm in some spermatids. **c** Control. **a', b', c'** represent the black and white images of **a**–**c**, respectively. Bars = 20 µm, for **a** and **c**; 10 µm, for **b**

Ye 2014). In addition, iRap1 testis histology documented another anomaly, i.e. the misorientation of groups of elongating spermatids with their heads positioned parallel to the basement membrane and/or pointing toward the tubule lumen (Suppl. Figure 2).

Partitioning of VEC and VEC Y658-phosphorylation

The shift from a strong to a weak state of cell–cell adhesion is known to result in an increase of VEC solubilisation under mild extraction conditions (Lampugnani et al. 1997). We thus checked for the level of mildly solubilized versus detergent-solubilized VEC from the seminiferous tubules of mice at different post-natal ages. In accordance with the proceeding of the first spermatogenic wave, seminiferous tubules of 25-day-old (P25) mice contain differentiating spermatids that are entering the acrosomal phase, while seminiferous tubules of 32-day-old (P32) mice have elongated spermatids next to initiate the process of spermiation (Bellvé et al. 1977). Mildly solubilized and detergent-solubilized protein extracts (see "Materials and methods" for detail) from P25 and P32 mice were analysed by VEC immunoblotting. Representative results are shown in Fig. 7a. The quantification of intensity of protein bands indicates that a larger amount of mildly solubilized (MS)- versus detergent-solubilized (DS)-VEC (approximately a MS/DS ratio of 0.83) was found in P32 seminiferous tubules in comparison to the P25 seminiferous tubules (approximately a MS/DS ratio of 0.32). This suggests that cumulatively at P32, VEC is more loosely associated to the plasma membrane and/or underlying cytoskeleton structure than at P25.

Tyrosine phosphorylation of VEC reflects an impairment of cell–cell contacts (Bravi et al. 2014; Giampietro 2016). In particular, phosphorylation at the tyrosine residue 658 (pY658) reduces VEC binding to p120 catenin that, consequently, cannot any longer function as signal for retention of VEC to the plasma membrane (Potter et al. 2005; Orsenigo et al. 2012; Cadwell et al. 2016). Moreover, at least in somatic cells phosphorylation of VEC at Y658 allows, by inducing dissociation of 120 catenin, binding of VEC to the polarity protein LGN (Conway et al. 2017). We considered that VEC becomes more loosely associated with the plasma membrane showing at the same time a progressive polarized cell compartmentalization as spermatids elongate.

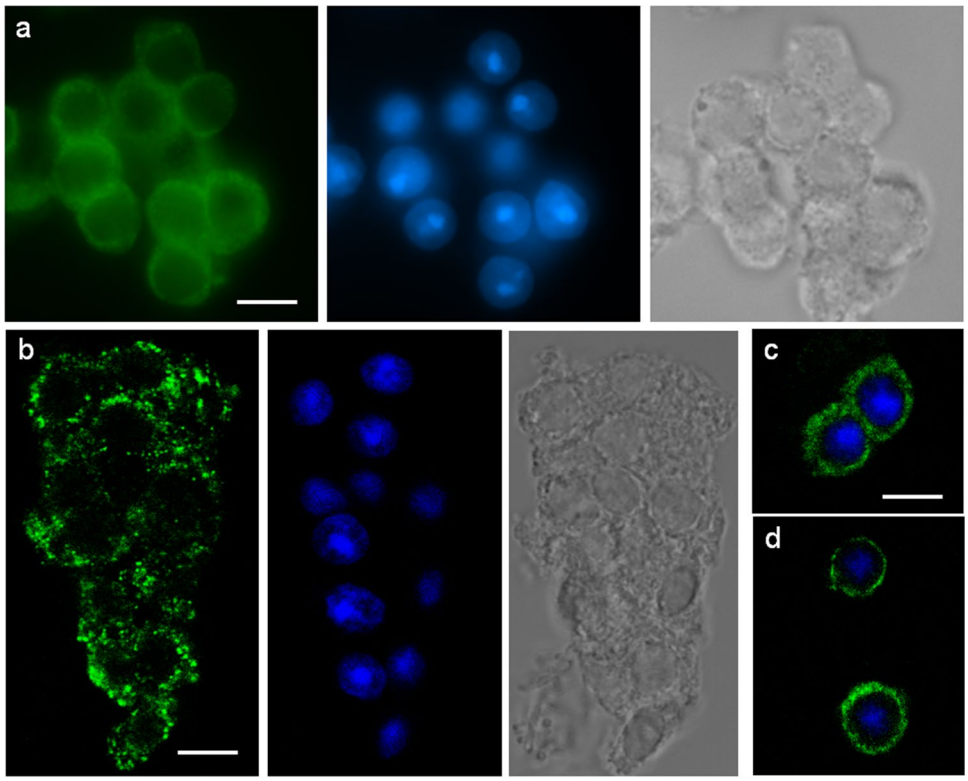

Fig. 4 VEC immunolabeling of round spermatids from fragmented testis material. **a**, **b** Seminiferous epithelial fragments (**b** was Triton X-100 pre-treated) labelled for VEC (left) and nuclei (middle) plus the respective phase contrast (right). **c**, **d** Spontaneously released round spermatids double labelled for VEC/DAPI. Bar = 12 µm

This prompted us to search for the presence of pY658-VEC in mouse testis. Protein extracts from pervanadate-treated seminiferous tubules of P25 and P32 mice were subjected to immunoprecipitation with the specific pY658-antibody that recognizes selectively the tyrosine phosphorylated at residue 658 of the murine VEC (Orsenigo et al. 2012). The immunoprecipitated proteins were then immunoblotted with VEC antibody. A higher amount of pY658-VEC (about 22% of total VEC) was detected in P32 seminiferous tubules than in P25 where the pY658-VEC was only 1.8% of total VEC (Fig. 7b). Lastly, we performed double pY658-VEC/sp56 fluorescent immunolabeling on cells released from testis fragments. pY658-VEC immunostaining was found to be essentially intracellular and with a pattern, in elongating spermatids, consistent with what we observed for VEC (Fig. 7c).

Discussion

Despite previous controversy about the presence of cadherin/catenin-based complexes in mammalian testis (Byers et al. 1994), more recently emerged evidence has confirmed the presence of a mosaic of cadherins and catenins in the seminiferous epithelium; cadherins, in particular, exhibit changes in their expression pattern depending on the stages of the epithelial cycle and the mammalian species examined (Goossens and van Roy 2005; Preissner and Bronson 2007). Here we provide novel evidence about the presence of VEC in mouse testis. Differently by the other testis cadherins so far described as a gene product of Sertoli cells, VEC is expressed by germ cells, in particular, round spermatids. The VEC relocation we unravelled during spermatid differentiation suggests that the cadherin, in addition to the adhesive function, may fulfil a role in acquisition of spermatid polarity and/or orientation inside the seminiferous epithelium.

Spermatogenesis could take place thanks to the intimate relationship between Sertoli and germ cells for which the cell–cell contacts are the mainstay. So far, the membrane-surface characterization of these contacts has been devoted essentially to Sertoli cells that represent the structural framework of the epithelium. Germ cells, however, are not only a passive mass that has to be transported anonymously. The timely and spatially organized sequence of cell differentiation and specialization events that typifies male germ cells, including the peculiarity of the few adhesion molecules identified till now in spermatids (Ozaki-Kuroda et al. 2002; Gliki et al. 2004; Inagaki et al. 2006; Wakayama et al. 2006), well documents that germ cells cannot be only rubbish. We thus need some more information about the germinal adhesion component.

To verify the effects of Rap1 silencing in vivo in germ cells, we generated previously a mouse iRap1 model (Aivatiadou et al. 2007). The more striking defect observed was the male sub-fertility due to the premature release of round spermatids from the Sertoli cells with consequent low counts

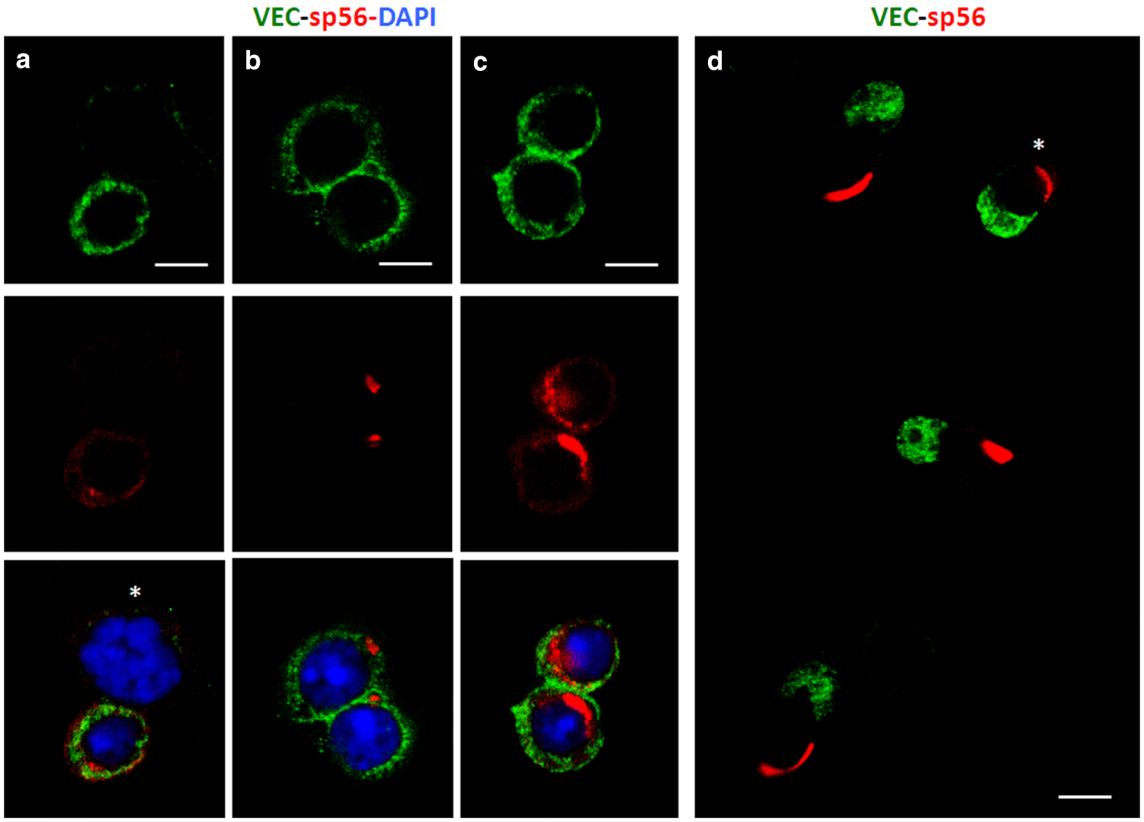

Fig. 5 Changes in VEC localization concomitantly to the acrosome biogenesis and spermatid elongation. **a**–**c** Columns. Round spermatids at different steps of differentiation, double immunolabeled for VEC (green) and sp56 (red) and counterstained with DAPI (merged triple labelling at the bottom strip). Note the VEC/sp56-negative primary spermatocyte (asterisk) in **a**. On the contrary, continuous VEC labelling signs the contour of round spermatids that, by exploiting sp56 staining pattern, can be staged as: at the Golgi phase (**a**), early cap phase (**b**) and late cap phase (**c**). Bars = 7 µm. **d** Massive relocation and internalization of VEC in spermatids at more advanced differentiation steps; in particular, elongating spermatid at the acrosomal phase (asterisk) and spermatids at different steps of the maturation phase. Bar = 10 µm

of mature spermatozoa. With VEC being a downstream target of Rap1 (Kooistra et al. 2007; Wilson and Ye 2014; Lakshmikanthan et al. 2015), we searched for VEC in the wild-type testis, unraveling that the cadherin is effectively expressed and with a pattern of localization restricted essentially to the apical compartment (Aivatiadou et al. 2007). In the present work, we show utilizing more approaches of immunolocalization, including mechanically isolated testis fragments and spontaneously released germ cells, that VEC is expressed at detectable level in post-meiotic male germ cells and is associated with the cellular membrane in round spermatids already when aES is not assembled yet. Apical ES first appears when spermatids start to elongate (steps 7–8); in step 8 spermatids, the acrosome has entered in the cap phase and the chromatin condensation is at the beginning. We found unexpectedly that in elongating spermatids VEC disappears just at the preferential site of aES assembling that is opposite to the forming acrosome, even if it persists in other plasma membrane domains. VEC is then completely internalized in elongated spermatids. It can be argued that VEC is not a component of the fully established aES, the only anchoring device that remains until the appearance of TBCs at spermiation; rather, its remarkable association with the round spermatid plasma membrane suggests that VEC could be involved in another type of Sertoli–spermatid contact, the so-called desmosome-like junction (Russell 1977). Ultrastructural studies carried out in the late 1970s and early 1980 reported in fact the existence of 'desmosome-like' structures between Sertoli cells and all non-elongating/elongated spermatids (for a review, see Goossens and van Roy 2005). Successively, these structures have been confirmed immunohistochemically by other authors (Byers et al. 1994; Johnson and Boekelheide 2002; Vogl et al. 2008; Cheng et al. 2011b), and resulted not conventional desmosomes notwithstanding the expression of desmosomal cadherins like desmoglein-2 and desmocollin-2 (Johnson and Boekelheide 2002; Vogl et al. 2000; Lie et al. 2010). For correctness of information, it is to mention, however, that there is not a general agreement on this topic. According to some researchers (Domke et al. 2014), the

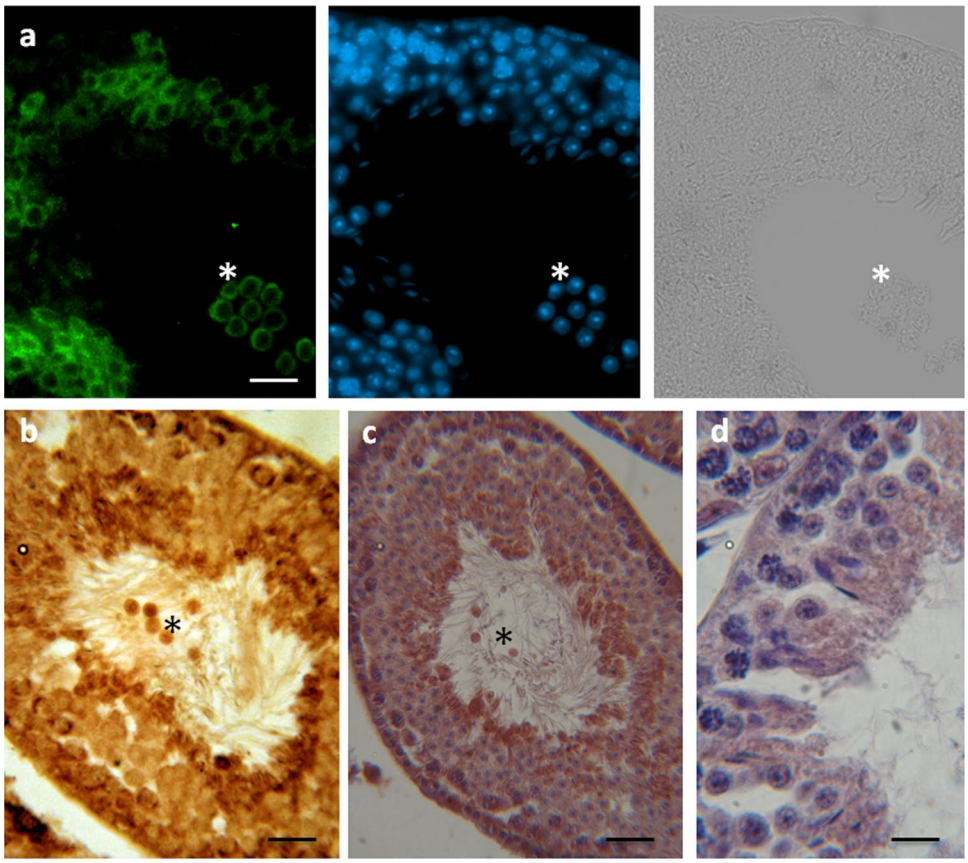

Fig. 6 VEC localization in the testis of transgenic iRap1 mice. Immunofluorescence (**a**) and immunoperoxidase (**b**–**d**) staining show VEC-immunopositivity inside the round spermatids prematurely released into the tubule lumen (asterisks). Even round spermatids still in situ have VEC-stained cytoplasm. **a** There are shown VEC, DAPI, and phase contrast, respectively. Bar = 20 µm. **b** VEC-immunoperoxidase staining only, whereas **c** and **d** were counterstained with haematoxylin. Bars = 25 µm for **b** and **c**, 15 µm for **d**

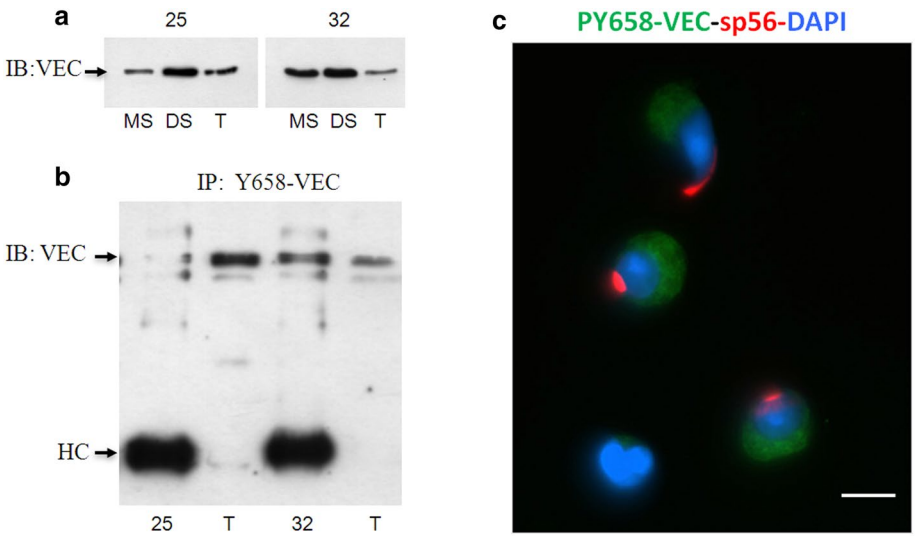

Fig. 7 Temporal correlation between VEC solubilisation and VEC Y658-phosphorylation at the first wave of spermatogenesis. **a** Representative images of VEC immunoblot (IB) analyses of mildly solubilized (MS) and detergent-solubilized (DS) protein extracts from the seminiferous epithelium of 25-day-old and 32-day-old mice; *T* is the respective total homogenate fraction (see "Material and methods" for details). **b** Representative image of VEC immunoblot (IB) analyses of pY658-VEC-precipitated immunocomplexes (IP) from the pervanadate-treated seminiferous epithelia of 25-day-old and 32-day-old mice; *T* (on the right side of the respective IP) is the total protein lysate input. HC indicates the antibody heavy chain (see "Material and methods" for details). **c** Double pY658-VEC/sp56 immunofluorescence analysis in spontaneously released spermatids from fragmented testis material, triple-stained with DAPI. No pY658-VEC surface labelling could be detected; conversely, pY658-VEC stains the cytoplasm opposing the developing acrosome in spermatids at different steps of differentiation. Bar = 7 µm

seminiferous tubules contain neither any desmosome structures nor any canonical desmosome-specific cadherins. At present, we have not any substantial evidence in support of one of the two opposing opinions. Immunohistochemistry and immunocytochemistry document that VEC is associated with round spermatid plasma membrane and is prone to disappear gradually from the membrane in elongating/elongated spermatids when aES stabilizes its assembling. It may be suggested that VEC could provide the joining ring between the conflicting results about the existence or not in the apical seminiferous epithelium of the two major types of cadherin-dependent cell–cell contacts, i.e. the adherens junction and the desmosome-like adhesion. It is indeed widely accepted that the specialized anchoring cell–cell adhesion in the testis can employ a functional unit different from the canonical adherens junction in epithelial cells (Byers et al. 1994; Goossens and van Roy 2005; Preissner and Bronson 2007). In addition, VEC is known to couple to both the actin and intermediate filament cytoskeleton in another type of peculiar junctional complex, the endothelial barrier (Kowalczyk et al. 1998).

In this regard, it is just the endothelial barrier the dynamic junction to which we referred in our previous study on iRap1 mice (Aivatiadou et al. 2007). Interfering with Rap1 function leads in fact to endothelial barrier impairment (Fukuhara et al. 2006; Wilson and Ye 2014; Lakshmikanthan et al. 2015). Accordingly, here we searched for VEC in iRap1 transgenic round spermatids finding that, in agreement with what occurs in endothelial cells, VEC is not plasma membrane-associated in these spermatids; consequently, these last can be easily prematurely released into the tubule lumen. This finding is explicative because it provides a significant in vivo proof of the importance of the VEC-mediated spermatid–Sertoli cell contacts. Always exploiting knowledge obtained from endothelial barrier biology, we planned some further experiments. Hallmarks of the loosening of VEC-mediated cell–cell contacts are the increase in VEC solubilization under mild extraction conditions (Lampugnani et al. 1997), and the increase in VEC-phosphorylation on tyrosine residues (Orsenigo et al. 2012; Sidibe and Imhof 2014; Schnittler 2016). We reasoned that during the physiological wave of the epithelial cycle, these two parameters could not remain constant, but, as suggested by immunocytochemical analysis, they have to increase in concomitance with the elongation of spermatids. By comparing protein extracts from the seminiferous epithelium of 25-day-old and 32-day-old mice that are both at their first spermatogenic wave, VEC resulted to be, in line with the expectations, more easily solubilizable in the seminiferous epithelium where elongated spermatids have made their appearance, i.e. that of 32-day-old mice. The other parameter to assay is VEC tyrosine-phosphorylation. According to the type of stimuli, specific tyrosine residues present at the cytoplasmic region of VEC become phosphorylated through the activation of non- receptor tyrosine kinases of the Src/src family kinases (SFKs) (Fukuhara et al. 2006; Orsenigo et al. 2012). Mouse germ cells express more SFK members (Berruti and Porzio 1992; Berruti and Borgonovo 1996; Xiao et al. 2014) while VEC has already been shown to undergo tyrosine phosphorylation in the seminiferous epithelium (Aivatiadou et al. 2007). Recently, Conway et al. (2017) have found that VEC phosphorylation at residue Y658 regulates endothelial barrier remodelling and physiology by promoting binding of pY658-VEC to the polarity protein LGN. With the acquisition of cell polarity being a distinctive feature of spermatid differentiation that influences also the polarized orientation in the seminiferous tubules, we searched for the presence of pY658-VEC by utilizing the pY658-VEC antibody used in the above-cited work of Conway et al. (2017). It was found that VEC can be phosphorylated on Y658; intriguingly, increase in the small pool of pY658-VEC keeps pace with the increase in VEC solubilization and spermatid elongation. These findings suggest that the triggering for VEC internalization just when aES assembles could be a signalling to promote another phenomenon, namely spermatid elongation. Indeed, cadherins have already been indicated to play a role in the transduction of signals (Bravi et al. 2014; Cadwell et al. 2016). Here we found that VEC, and in particular the pool of pY658-VEC, goes to compartmentalize towards the developing spermatid distal pole where most organelles like the Golgi complex and centrioles also move. VEC, under the form of a VEC–PAR3–alpha-catenin complex, has been shown to regulate Golgi localization in somatic cells (Odell et al. 2012) as well as JAM-C, a junction adhesion molecule expressed in the testis by spermatids but not Sertoli cells, is involved in spermatid polarization by recruiting proteins of the Par6, Cdc42, PKCλ cell polarity complex (Gliki et al. 2004; Cartier-Michaud et al. 2017). Work addressed to verify a possible involvement of VEC in spermatid polarization is next to be engaged in our laboratory.

Acknowledgements The authors are grateful to Prof. E. Dejana and Dr. C. Giampietro (from the IFOM, FIRC Institute of Molecular Oncology, Milano, Italy) for the anti-pY658VEC antibody and to Dr. C. Paiardi (Dept. Biosciences, Univ. Milano, Italy) for assistance with fluorescence microscopy. This work was supported by grants from Transition Grant 2012, University of Milano to G.B.

Compliance with ethical standards

Conflict of interest None of the authors have financial or other types of competing interests.

References

Aivatiadou E, Mattei E, Ceriani M, Tilia L, Berruti G (2007) Impaired fertility and spermiogenetic disorders with loss of cell adhesion

in male mice expressing an interfering Rap1 mutant. Mol Biol Cell 18(4):1530–1542
Aivatiadou E, Ripolone M, Brunetti F, Berruti G (2009) cAMP-Epac2-mediated activation of Rap1 in developing male germ cells: RA-RhoGAP as a possible direct down-stream effector. Mol Reprod Dev 76(4): 407–416. https://doi.org/10.1002/mrd.20963
Bartolomé RA, Torres S, Isern de Val S, Escudero-Paniagua B, Calviño E, Teixidó J (2017) Casal JI VE-cadherin RGD motifs promote metastasis and constitute a potential therapeutic target in melanoma and breast cancers. Oncotarget 8(1):215–227. https://doi.org/10.18632/oncotarget.13832
Bellvé AR, Cavicchia JC, Millette CF, O'Brien DA, Bhatnagar YM, Dym M (1977) Spermatogenic cells of the prepuberal mouse. Isolation and morphological characterization. J Cell Biol 74(1):86–97
Berruti G (2000) A novel rap1/B-Raf/14-3-3 theta protein complex is formed in vivo during the morphogenetic differentiation of post-meiotic male germ cells. Exp Cell Res 257(1):172–179
Berruti G, Borgonovo B (1996) sp42, the boar sperm tyrosine kinase, is a male germ cell-specific product with a highly conserved tissue expression extending to other mammalian species. J Cell Sci 109(Pt 4):851–858
Berruti G, Paiardi C (2014) The dynamic of the apical ectoplasmic specialization between spermatids and Sertoli cells: the case of the small GTPase Rap1. Biomed Res Int 2014:635979. https://doi.org/10.1155/2014/635979
Berruti G, Paiardi C (2015) USP8/UBPy-regulated sorting and the development of sperm acrosome: the recruitment of MET. Reproduction 149(6): 633 – 44. https://doi.org/10.1530/REP-14-0671
Berruti G, Porzio S (1992) Tyrosine protein kinase in boar spermatozoa: identification and partial characterization. Biochim Biophys Acta 1118(2):149–154
Bravi L, Dejana E, Lampugnani MG (2014) VE-cadherin at a glance. Cell Tissue Res 355: 515 – 22
Byers SW, Sujarit S, Jegou B, Butz S, Hoschutzky H, Herrenknecht K, MacCalman C, Blaschuk OW (1994) Cadherins and cadherin-associated molecules in the developing and maturing rat testis. Endocrinology 134(2):630–639
Cadwell CM, Su W, Kowalczyk AP (2016) Cadherin tales: Regulation of cadherin function by endocytic membrane trafficking. Traffic 17(12):1262–1271
Cartier-Michaud A, Bailly AL, Betzi S, Shi X, Lissitzky JC, Zarubica A, Sergé A, Roche P, Lugari A, Hamon V, Bardin F, Derviaux C, Lembo F, Audebert S, Marchetto S, Durand B, Borg JP, Shi N, Morelli X, Aurrand-Lions M (2017) Genetic, structural, and chemical insights into the dual function of GRASP55 in germ cell Golgi remodeling and JAM-C polarized localization during spermatogenesis. PLoS Genet 13(6):e1006803. https://doi.org/10.1371/journal.pgen.1006803
Cheng CY, Lie PP, Mok KW, Cheng YH, Wong EW, Mannu J, Mathur PP, Yan HH, Mruk DD (2011a) Interactions of laminin β3 fragment with β1-integrin receptor: a revisit of the apical ectoplasmic specialization-blood-testis-barrier-hemidesmosome functional axis in the testis. Spermatogenesis 1(3):174–185
Cheng CY, Wong EWP, Lie PPY, Li MWM, Mruk DD, Yan HHN, Mok D-W, Mannu J, Mathur PP, W-y L, Bonanomi M, Silvestrini B (2011b) Regulation of blood-testis barrier dynamics by desmosome, gap junction, hemidesmosome and polarity proteins. An unexpected turn of events. Spermatogenesis 1:105–115
Combes AN, Wilhelm D, Davidson T, Dejana E, Harley V, Sinclair A, Koopman P (2009) Endothelial cell migration directs testis cord formation. Dev Biol 326:112–120
Conway DE, Coon BG, Budatha M, Arsenovic PT, Orsenigo F, Wessel F, Zhang J, Zhuang Z, Dejana E, Vestweber D, Schwartz MA (2017) VE-cadherin phosphorylation regulates endothelial fluid shear stress responses through the polarity protein LGN. Curr Biol 27:2219–2225
Di Lorenzo A, Lin MI, Murata T, Landskroner-Eiger S, Schleicher M, Kothiya M, Iwakiri Y, Yu J, Huang PL, Sessa WC (2013) eNOS-derived nitric oxide regulates endothelial barrier function through VE-cadherin and Rho GTPases. J Cell Sci 126(Pt 24):5541–5552. https://doi.org/10.12422/jcs.115972
Domke LM, Rickelt S, Dörflinger Y, Kuhn C, Winter-Simanowski S, Zimbelmann R, Rosin-Arbesfeld R, Heid H, Franke WW (2014) The cell-cell junctions of mammalian testes: I. The adhering junctions of the seminiferous epithelium represent special differentiation structures. Cell Tissue Res 357(3):645–665. https://doi.org/10.1007/s00441-014-1906-9
Fukuhara S, Sakurai A, Yamagishi A, Sako K, Mochizuki N (2006) Vascular endothelial cadherin-mediated cell-cell adhesion regulated by a small GTPase, Rap1. J Biochem Mol Biol 39(2):132–139
Giampietro C (2016) VE-cadherin complex plasticity: EPS8 and YAP play relay at adherens junctions. Tissue Barriers 4(4):e1232024. https://doi.org/10.1080/21688370.2016.1232024
Gliki G, Ebnet K, Aurrand-Lions M, Imhof BA, Adams RH. Nature Gliki G, Ebnet K, Aurrand-Lions M, Imhof BA, Adams RH (2004) Spermatid differentiation requires the assembly of a cell polarity complex downstream of junctional adhesion molecule-C. Spermatid differentiation requires the assembly of a cell polarity complex downstream of junctional adhesion molecule-C. Nature 431(7006):320–324
Goossens S, van Roy F (2005) Cadherin-mediated cell-cell adhesion in the testis. Front Biosci 10:398–419
Guttman JA, Takai Y, Vogl AW (2004) Evidence that tubulobulbar complexes in the seminiferous epithelium are involved with internalization of adhesion junctions. Biol Reprod 71:548–559
Inagaki M, Irie K, Ishizaki H, Tanaka-Okamoto M, Miyoshi J, Takai Y (2006) Role of cell adhesion molecule nectin-3 in spermatid development. Genes Cells 11(9):1125–1132
Johnson KJ, Boekelheide K (2002) Dynamic testicular adhesion junctions are immunologically unique. II. Localization of classic cadherins in rat testis. Biol Reprod 66:992–1000
Kooistra MR, Dube N, Bos JL (2007) Rap1: a key regulator in cell-cell junction formation. J Cell Sci 120:17–22. https://doi.org/10.1242/jcs.03306
Kowalczyk AP, Navarro P, Dejana E, Bornslaeger EA, Green KJ, Kopp DS, Borgwardt JE (1998) VE-cadherin and desmoplakin are assembled into dermal microvascular endothelial intercellular junctions: a pivotal role for plakoglobin in the recruitment of desmoplakin to intercellular junctions. J Cell Sci 111(Pt 20):3045–3057
Lakshmikanthan S, Zheng X, Nishijima Y, Sobczak M, Szabo A, Vasquez-Vivar J, Zhang DX, Chrzanowska-Wodnicka M (2015) Rap1 promotes endothelial mechanosensing complex formation, NO release and normal endothelial function. EMBO Rep 16:628–637
Lampugnani MG, Corada M, Andriopoulou P, Esser S, Risau W, Dejana E (1997) Cell confluence regulates tyrosine phosphorylation of adherens junction components in endothelial cells. J Cell Biol 110:2065–2077
Li N, Mruk DD, Wong CK, Lee WM, Han D, Cheng CY (2015) Actin-bundling protein plastin 3 is a regulator of ectoplasmic specialization dynamics during spermatogenesis in the rat testis. FASEB J 29(9):3788–3805. https://doi.org/10.1096/fj.14-267997
Lie PPY, Cheng CY, Mruk DD (2010) Crosstalk between desmoglein-2/ desmocollin-2/Src kinase and Coxsackie and adenovirus receptor/ ZO-1 protein complexes regulates blood-testis barrier dynamics. Int J Biochem Cell Biol 42:975–986
Mulholland DJ, Dedhar S, Vogl AW (2001) Rat seminiferous epithelium contains a unique junction (ectoplasmic specialization) with signaling properties both of cell/cell and cell/matrix junctions. Biol Reprod 64:396–407

Nicholls PK, Harrison CA, Walton KL, McLachlan RI, O'Donnell L, Stanton PG (2011) Hormonal regulation of Sertoli cell microRNAs at sprmiation. Endocrinology 152(4):1670–1683. https://doi.org/10.1210/en.2010-1341

Noda K, Zhang J, Fukuhara S, Kunimoto S, Yoshimura M, Mochizuki N (2010) Vascular endothelial-cadherin stabilizes at cell-cell junctions by anchoring to circumferential actin bundles through alpha- and beta-catenins in cyclic AMP-Epac-Rap1 signal-activated endothelial cells. Mol Biol Cell 21(4):584–596. https://doi.org/10.1091/mbc.E09-07-0580

Oakberg EF (1956) Duration of spermatogenesis in the mouse and timing of stages of the cycle of the seminiferous epithelium. Am J Anat 99(3):507–516

O'Donnell L, Nicholls PK, O'Bryan MK, McLachlan RI, Stanton PG (2011) Spermiation: the process of sperm release. Spermatogenesis 1:14–35

Odell AF, Hollstein M, Ponnambalam S, Walker JH (2012) A VE-cadherin-PAR3-α-catenin complex regulates the Golgi localization and activity of cytosolic phospholipase A(2)α in endothelial cells. Mol Biol Cell 23(9):1783–1796. https://doi.org/10.1091/mbc.E11-08-0694

Orsenigo F, Giampietro C, Ferrari A, Corada M, Galaup A, Sigismund S, Ristagno G, Maddaluno L, Koh GY, Franco D, Kurtcuoglu V, Poulikakos D, Baluk P, McDonald D, Grazia Lampugnani M, Dejana E (2012) Phosphorylation of VE-cadherin is modulated by haemodynamic forces and contributes to the regulation of vascular permeability in vivo. Nat Commun 3:1208. https://doi.org/10.1038/ncomms2199

Ozaki-Kuroda K, Nakanishi H, Ohta H, Tanaka H, Kurihara H, Mueller S, Irie K, Ikeda W, Sakai T, Wimmer E, Nishimune Y, Takai Y (2002) Nectin couples cell-cell adhesion and the actin scaffold at heterotypic testicular junctions. Curr Biol 12:1145–1150

Paiardi C, Pasini ME, Gioria M, Berruti G (2011) Failure of acrosome formation and globozoospermia in the wobbler mouse, a Vps54 spontaneous recessive mutant. Spermatogenesis 1(1):52–62

Paiardi C, Pasini ME, Amadeo A, Gioria M, Berruti G (2014) The ESCRT-deubiquitinating enzyme USP8 in the cervical spinal cord of wild-type and Vps54-recessive (wobbler) mutant mice. Histochem Cell Biol 141(1):57–73. https://doi.org/10.1007/s00418-013-1096-7

Potter MD, Barbero S, Cheresh DA (2005) Tyrosine phosphorylation of VE-cadherin prevents binding of p120- and beta-catenin and maintains the cellular mesenchymal state. J Biol Chem 280(36):31906–31912

Preissner KT, Bronson RA (2007) The role of multifunctional adhesion molecules in spermatogenesis and sperm function: Lessons from hemostasis and defense? Semin Thromb Hemost 33(1):100–110

Pronk MCA, van Bezu JSM, van Nieuw Amerongen GP, van Hinsbergh VWM, Hordijk PL (2017) RhoA, RhoB and RhoC differentially regulate endothelial barrier function. Small GTPases. https://doi.org/10.1080/21541248.2017.1339767

Russell LD (1977) Desmosome-like junctions between Sertoli and germ cells in the rat testis. Am J Anat 148:301–312

Russell LD, Lee IP, Ettlin R, Peterson RN (1983) Development of the acrosome and alignment, elongation and entrenchment of spermatids in procarbazine-treated rats. Tissue Cell 15(4):615–626

Schnittler H (2016) Contraction of endothelial cells: 40 years of research, but the debate still lives. Histochem Cell Biol 146(6):651–656

Sidibe A, Imhof BA (2014) VE-cadherin phosphorylation decides: vascular permeability or diapedesis. Nat Immunol 15: 215——217

Suzuki S, Sano K, Tanihara H (1991) Diversity of the cadherin family: evidence for eight new cadherins in nervous tissue. Cell Regul 2:261–270

Vogl AW, Pfeiffer DC, Mulholland D, Kimel G, Guttman J (2000) Unique and multifunctional adhesion junctions in the testis: ectoplasmic specializations. Arch Histol Cytol 63(1):1–15

Vogl AW, Vaid KS, Guttman JA (2008) The Sertoli cell cytoskeleton. Adv Exp Med Biol 636:186–211

Wakayama T, Koami H, Ariga H, Kobayashi D, Sai Y, Tsuji A, Yamamoto M, Iseki S (2003) Expression and functional characterization of the adhesion molecule spermatogenic immunoglobulin superfamily in the mouse testis. Biol Reprod 68:1755–1763L

Wen Q, Tang EI, Xiao X, Gao Y, Chu DS, Mruk DD, Silvestrini B, Cheng CY (2016) Transport of germ cells across the seminiferous epithelium during spermatogenesis—the involvement of both actin- and microtubule-based cytoskeletons. Tissue Barriers 4:e1265042. https://doi.org/10.1080/21688370.2016.1265042

Wilson CW, Ye W (2014) Regulation of vascular endothelial junction stability and remodeling through Rap1-Rasip1 signaling. Cell Adh Migr 8(2):76–83

Xiao K, Garner J, Buckley KM, Vincent PA, Chiasson CM, Dejana E, Faundez V, Kowalczyk AP (2005) p120-Catenin regulates clathrin-dependent endocytosis of VE-cadherin. Mol Biol Cell 16(11):5141–5151

Xiao X, Mruk D, Wong CKC, Cheng CY (2014) Germ cell transport across the seminiferous epithelium during spermatogenesis. Physiol 29:286–298

Yamada D, Yoshida M, Williams YN, Fukami T, Kikuchi S, Masuda M, Maruyama T, Ohta T, Nakae D, Maekawa A, Kitamura T, Murakami Y (2006) Disruption of spermatogenic cell adhesion and male infertility in mice lacking **TSLC1**/IGSF4, an immunoglobulin superfamily cell adhesion molecule. Mol Cell Biol 26(9):3610–3624

Young JS, Guttman JA, Vaid KS, Vogl AW (2009) Tubulobulbar complexes are intercellular podosome-like structures that internalize intact intercellular junctions during epithelial remodeling events in the rat testis. Biol Reprod 80:162–174